

## Interaction potentials and momentum transfer in ionic collisions: Uranium

James S. Cohen\*

*Theoretical Division, Los Alamos Scientific Laboratory, University of California, Los Alamos, New Mexico 87545*

(Received 4 June 1979)

The effect of elastic collisions of  $U^+$  with  $U$ ,  $U^+$ , and  $U^{2+}$  in a  $U^+$  plasma has been investigated. The required potential-energy curves were calculated by means of the electron-gas (Gordon-Kim-Rae) statistical method. An effective polarization potential was added to the ion-neutral potential curve. Collisional phase shifts were evaluated by the semiclassical JWKB method using a very efficient algorithm. Modifications necessary to take into account the long-range shielded Coulomb potential in ion-ion collisions are described. Momentum-transfer and viscosity cross sections, without charge transfer, are presented and their dependences on the long- and short-range potentials are examined.

### I. INTRODUCTION

Momentum transfer in collisions is an important characteristic of plasmas. The momentum-transfer cross section for an unshielded Coulomb potential is well known to be infinite, so that when ion-ion scattering is treated, the Debye shielding of the plasma must be taken into account to obtain a long-range potential of the form

$$V(R) \sim (Q_a Q_b / R) \exp(-R/\lambda_{De}), \quad (1)$$

where  $Q_a$  and  $Q_b$  are the ionic charges and  $\lambda_{De}$  is the shielding length. Momentum transfer is dominated at low collision energies by the long-range (though shielded) Coulomb potential and at relatively high energies by the short-range repulsive potential. In the absence of detailed knowledge of the ion interaction potentials, the collision integrals, which, for example, result from expansion of the collision term of the Boltzmann equation in powers of the momentum transfer for a two-body collision or from the Fokker-Planck equation,<sup>1</sup> are often approximated by arbitrarily neglecting the small-angle and large-angle scattering. When a complete interaction potential has been available, the differential scattering cross section has usually been calculated through the classical deflection angle.

In the present work, we show that theoretical developments of recent years make possible efficient calculation of interaction potentials using electron-gas methods and of relevant collision properties using the semiclassical JWKB method. These procedures should be relatively accurate for ion-ion or ion-neutral collisions typical of many plasmas. The present application is to  $U$  II-U I,  $U$  II-U II, and  $U$  II-U III collisions in a  $U^+$  plasma. First-order momentum-transfer (diffusion) and second-order momentum-transfer (viscosity) cross sections have been calculated. The sensitivities of the ion-ion cross sections to

the Debye shielding length and of the ion-neutral cross sections to the polarization-potential cutoff are discussed.

This work is mainly concerned with direct momentum transfer. Indirect momentum transfer, by way of resonant charge transfer in  $U$  II-U I and  $U$  II-U III collisions, depends mainly on the long-range exchange interaction and has been treated satisfactorily using asymptotic theories.

### II. INTERACTION POTENTIALS

#### A. Electron-gas model

The potential interactions were calculated using a modified electron-gas model, which has become well known as the Gordon-Kim method,<sup>2</sup> including a correction to the exchange energy by Rae.<sup>3</sup> The Gordon-Kim-Rae (GKR) method has been quite successful in determining complete potential curves between closed-shell atoms and short-range interactions between other species.<sup>4</sup> A few additional modifications are required for satisfactory treatment of dispersion interactions,<sup>5</sup> but these do not concern us in the present work. The GKR method requires as input only the unperturbed charge densities of the isolated species whose interaction is considered. The basic assumptions of the method are the following. (i) Each atom (or ion) is represented by its electronic charge density. (ii) The charge densities ( $\rho_a$  and  $\rho_b$ ) are assumed to be simply additive. (iii) The Coulomb electrostatic potential is calculated directly. (iv) The kinetic, exchange, and correlation energies are calculated using functionals obtained for a uniform, nonrelativistic electron gas. The exchange energy is multiplied by a correction factor to eliminate self-energy contributions which can be significant if the number of electrons is small. The second assumption is the most drastic and limits the method to closed-shell inter-

actions; within this limitation, however, Nikulin and Tsarev<sup>6</sup> have shown that the assumption is reasonable even in the united-atom limit.

The total interaction energy is then

$$V_{\text{GKR}}(R) = V_c(R) + V_{\text{eg}}(R). \quad (2)$$

The Coulomb interaction for two atoms (or ions) with nuclear charges  $Z_a$  and  $Z_b$  is given by

$$V_c = \frac{Z_a Z_b}{R} + \int \int d^3r_1 d^3r_2 \frac{\rho_a(\vec{r}_1) \rho_b(\vec{r}_2)}{r_{12}} - Z_b \int d^3r_1 \frac{\rho_a(\vec{r}_1)}{r_{1b}} - Z_a \int d^3r_2 \frac{\rho_b(\vec{r}_2)}{r_{2a}}. \quad (3a)$$

To avoid a large degree of cancellation between

$$V_c(R) = \frac{Q_a Q_b}{R} + \int_0^\infty dr_1 4\pi r_1^2 \rho_a(r_1) \int_0^\infty dr_2 4\pi r_2^2 \rho_b(r_2) \left( \frac{Z_a Z_b - Q_a Q_b}{(Z_a - Q_a)(Z_b - Q_b)} \frac{1}{R} - \frac{2Z_b}{Z_b - Q_b} \frac{1}{R + r_1 + |R - r_1|} - \frac{2Z_a}{Z_a - Q_a} \frac{1}{R + r_2 + |R - r_2|} + F(R, r_1, r_2) \right), \quad (4)$$

where

$$F(R, r_1, r_2) = \begin{cases} 2/(R + r_1 + |R - r_1|), & \text{for } r_2 \leq |R - r_1| \\ \frac{1}{2} \left( \frac{1}{r_1} + \frac{1}{r_2} \right) - \frac{R}{4r_1 r_2} - \frac{(r_1 - r_2)^2}{4Rr_1 r_2}, & \text{for } |R - r_1| < r_2 < R + r_1 \\ 1/r_2, & \text{for } r_2 \geq R + r_1. \end{cases} \quad (5)$$

The double integral in Eq. (4) is accurately done by Gauss-Legendre quadrature. The radial distance was segmented with  $\Delta r = 10a_0$  and 100 quadrature points were taken in each segment (fewer points would have been adequate). In all cases the integral was well converged by  $r_a$  (or  $r_b$ ) =  $15a_0$ . We may note here that the Gauss-Legendre quadrature was found to be more accurate than Gauss-Laguerre quadrature with a similar number of points.

If one ion is fully stripped (say  $Q_b = Z_b$ , for definiteness) then Eq. (4) is replaced simply by

$$V_c'(R) = \frac{Q_a Z_b}{R} + Z_b \int_0^\infty dr_1 4\pi r_1^2 \rho_a(r_1) \times \left( \frac{1}{R} - \frac{2}{R + r_1 + |R - r_1|} \right). \quad (4')$$

The non-Coulomb electron-gas interaction energy is given by

$$V_{\text{eg}}(R) = \int d^3r [(\rho_a + \rho_b) E_{\text{eg}}(\rho_a + \rho_b) - \rho_a E_{\text{eg}}(\rho_a) - \rho_b E_{\text{eg}}(\rho_b)]. \quad (6)$$

integrals, Eq. (3a) can be rearranged

$$V_c(R) = \frac{Q_a Q_b}{R} + \int \int d^3r_1 d^3r_2 \rho_a(\vec{r}_1) \rho_b(\vec{r}_2) \times \left( \frac{Z_a Z_b - Q_a Q_b}{(Z_a - Q_a)(Z_b - Q_b)} \frac{1}{R} - \frac{Z_b}{Z_b - Q_b} \frac{1}{r_{1b}} - \frac{Z_a}{Z_a - Q_a} \frac{1}{r_{2a}} + \frac{1}{r_{12}} \right), \quad (3b)$$

where  $Q_a$  and  $Q_b$  are the net ionic charges (assuming  $Q_a \neq Z_a$  and  $Q_b \neq Z_b$ ). This can be reduced to a two-dimensional integration<sup>2</sup> if  $\rho_a$  and  $\rho_b$  are each spherically symmetric; in that case,

The electron-gas functional (in Hartree atomic units) for  $N(N = Z_a + Z_b - Q_a - Q_b)$  electrons can be written

$$E_{\text{eg}} = E_{\text{kin}} + C_x(N) E_{\text{exch}} + E_{\text{corr}}, \quad (7)$$

where

$$E_{\text{kin}} = \frac{3}{10} (3\pi^2)^{2/3} \rho^{2/3}, \quad (8)$$

$$E_{\text{exch}} = -\frac{3}{4} (3/\pi)^{1/3} \rho^{1/3}, \quad (9)$$

$$E_{\text{corr}} = \begin{cases} 0.0311 \ln r_s - 0.048 + 0.009 r_s \ln r_s - 0.01 r_s, & \text{for } r_s \leq 0.7 \\ -0.06156 + 0.01898 \ln r_s, & \text{for } 0.7 < r_s < 10 \\ -0.438 r_s^{-1} + 1.325 r_s^{-3/2} - 1.47 r_s^{-2} - 0.4 r_s^{-5/2}, & \text{for } r_s \geq 10 \end{cases} \quad (10)$$

in terms of the radius

$$r_s = (3/4\pi\rho)^{1/3}, \quad (11)$$

and

$$C_x(N) = 1 - \frac{8}{3} \delta + 2\delta^2 - \frac{1}{3} \delta^4, \quad (12)$$

with  $\delta$  such that

$$\delta^3 (1 - \frac{8}{3} \delta + \frac{1}{4} \delta^3) = (4N)^{-1}. \quad (13)$$

The integral in Eq. (6) is more conveniently done in prolate spheroidal coordinates, for which

$$r_a = \frac{1}{2} (\xi + \eta) R, \quad (14a)$$

$$r_b = \frac{1}{2} (\xi - \eta) R, \quad (14b)$$

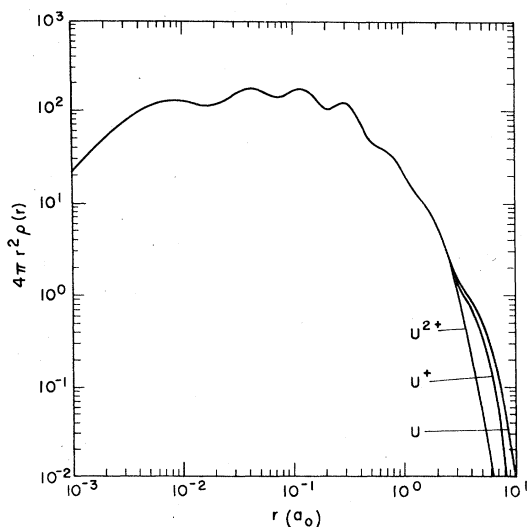


FIG. 1. Charge densities (multiplied by  $4\pi r^2$ ) for the ground-state configurations of U,  $U^+$ , and  $U^{2+}$ .

TABLE I. Potential energies obtained using the GKR method.

| $R(a_0)^a$ | $U^- - U^c$ | $V(\text{a.u.})^b$ |                |
|------------|-------------|--------------------|----------------|
|            |             | $U^+ - U^+$        | $U^+ - U^{2+}$ |
| 0.25       | 8959        | 8960               | 8960           |
| 0.50       | 1824        | 1825               | 1825           |
| 0.75       | 581.1       | 581.4              | 581.7          |
| 1.00       | 238.6       | 238.9              | 239.2          |
| 1.25       | 111.3       | 111.6              | 111.8          |
| 1.50       | 56.70       | 57.00              | 57.20          |
| 1.75       | 30.65       | 30.95              | 31.15          |
| 2.00       | 17.50       | 17.79              | 17.99          |
| 2.25       | 10.50       | 10.79              | 10.99          |
| 2.50       | 6.550       | 6.827              | 7.028          |
| 2.75       | 4.196       | 4.464              | 4.665          |
| 3.00       | 2.733       | 2.992              | 3.196          |
| 3.25       | 1.787       | 2.039              | 2.251          |
| 3.50       | 1.231       | 1.471              | 1.679          |
| 3.75       | 0.8511      | 1.081              | 1.287          |
| 4.00       | 0.5721      | 0.7950             | 1.005          |
| 4.25       | 0.4123      | 0.6251             | 0.8268         |
| 4.50       | 0.2898      | 0.4945             | 0.6927         |
| 4.75       | 0.2000      | 0.3977             | 0.5935         |
| 5.00       | 0.1473      | 0.3365             | 0.5250         |
| 5.50       | 0.0732      | 0.2487             | 0.4272         |
| 6.00       | 0.0337      | 0.1974             | 0.3652         |
| 6.50       | 0.0157      | 0.1679             | 0.3239         |
| 7.00       | 0.0060      | 0.1483             | 0.2935         |
| 7.50       | 0.0010      | 0.1345             | 0.2701         |
| 8.00       | -0.0013     | 0.1243             | 0.2513         |
| 8.50       | -0.0020     | 0.1164             | 0.2356         |
| 9.00       | -0.0022     | 0.1097             | 0.2221         |
| 9.50       | -0.0020     | 0.1040             | 0.2103         |
| 10.00      | -0.0017     | 0.0989             | 0.1998         |

<sup>a</sup>  $1a_0 = 0.52918 \text{ \AA}$ .

<sup>b</sup>  $1 \text{ a.u.} = 27.21 \text{ eV}$ .

<sup>c</sup> Does not include polarization potential.

and

$$d^3r = \frac{1}{8} R^3 (\xi^2 - \eta^2) d\phi d\eta d\xi. \quad (15)$$

The  $\phi$  integral is trivial and yields a factor of  $2\pi$ . The  $\xi$  integral was performed the same way as the radial integrals in Eq. (4); the  $\eta$  integral was performed using 32-point Gauss-Legendre quadrature.

### B. Results for uranium

The charge densities were calculated with numerical relativistic Hartree-Fock wave functions for the ground-state configurations,  $U(5f^3 6d^1 7s^2)$ ,  $U^+(5f^3 7s^2)$ , and  $U^{2+}(5f^3 6d^1)$ , using the program of Cowan and Griffin.<sup>7</sup> The one-electron wave functions represent an average over the component fine-structure levels and are thus spherically symmetric. These charge densities, shown in Fig. 1 (in a.u.,  $e = 1$ ), were then used in the GKR method described above to obtain the potential energies given in Table I. The use of the nonrelativistic electron-gas model with relativistic charge densities is not inconsistent since we are mainly concerned with interactions involving shells where the only significant relativistic effects are due to orthogonality constraints and are hence taken into account by the atomic charge densities. We note that in the present calculations  $C_x \approx 0.72$  in Eq. (7). The separate contributions to the GKR energy are given in Table II for the  $U^+ - U^+$  interaction. The procedure was repeated using densities for the low-lying excited states  $U^+(5f^3 6d^1 7s^1)$  and  $U^{2+}(5f^3 7s^1)$ , but the differences in the results were not considered important for present purposes.

The GKR potential curves for the ion-ion interactions already include all essential contributions, but the GKR potential curve for the ion-neutral interaction does not include the important contribution of induced polarization since the charge dis-

TABLE II. Components of the GKR energy for the  $U^+ - U^+$  interaction.

| $R(a_0)$ | Energy (a.u.) |         |                       |             |
|----------|---------------|---------|-----------------------|-------------|
|          | Coulomb       | Kinetic | Exchange <sup>a</sup> | Correlation |
| 0.5      | 525.4         | 1329.5  | -29.7                 | -0.6        |
| 1.0      | -15.68        | 265.00  | -10.06                | -0.31       |
| 2.0      | -11.32        | 31.44   | -2.22                 | -0.11       |
| 3.0      | -2.145        | 5.849   | -0.662                | -0.049      |
| 4.0      | -0.6064       | 1.6796  | -0.2526               | -0.0257     |
| 5.0      | -0.1268       | 0.5897  | -0.1118               | -0.0146     |
| 6.0      | 0.0486        | 0.2089  | -0.0516               | -0.0085     |
| 7.0      | 0.1047        | 0.0724  | -0.0239               | -0.0049     |
| 8.0      | 0.1132        | 0.0250  | -0.0111               | -0.0028     |
| 9.0      | 0.1076        | 0.0087  | -0.0051               | -0.0015     |
| 10.0     | 0.0990        | 0.0030  | -0.0023               | -0.0008     |

<sup>a</sup> Includes Rae correction factor  $C_x(182) = 0.7165$ .

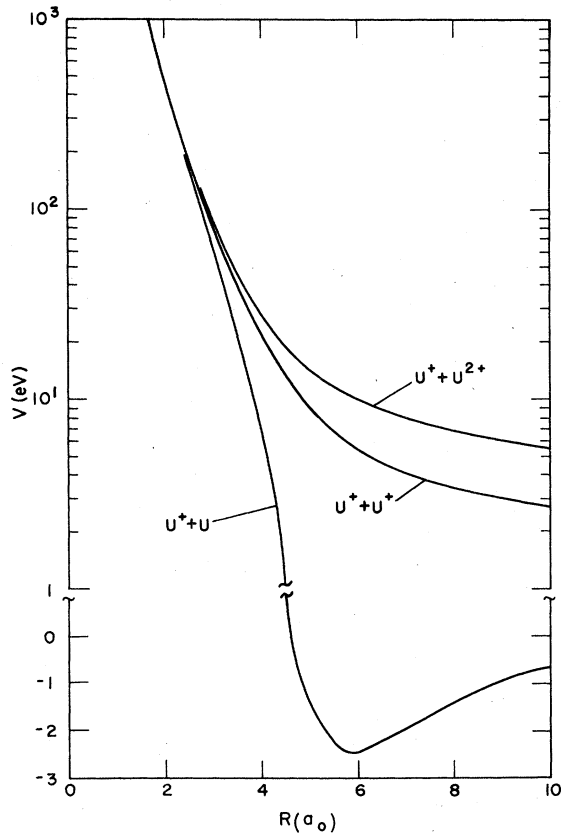


FIG. 2. Potential energy curves for  $U^+ + U$ ,  $U^+ + U^+$ , and  $U^+ + U^{2+}$ .

tributions were fixed. To take into account the polarization contribution to the latter, the potential is written

$$V(R) = V_{\text{GKR}}(R) - (\alpha/2R^4)f_4(R/R_0), \quad (16)$$

where

$$f_n(x) = 1 - e^{-x} \sum_{k=0}^n \frac{x^k}{k!} \quad (17)$$

is a cutoff function analogous to that obtained in the polarized-orbital method for electron scattering.<sup>8</sup> Note that  $f_4(x)/x^4 \sim x/120 \rightarrow 0$  as  $x \rightarrow 0$ . The dipole polarizability  $\alpha$  of U I has been determined in numerical Hartree-Fock calculations<sup>9</sup> to be  $66.0 \text{ \AA}^3$ . The potential curve for the  $U^+ - U$  interaction assuming  $R_0 = 1$  is shown in Fig. 2. This value of  $R_0$  will be shown in Sec. IIIB to be a reasonable choice.

### III. COLLISIONS

#### A. Semiclassical treatment

For the collision of two atoms (possibly one or both ionized) the momentum transfer (or diffusion) and viscosity cross sections are given in terms

of the differential cross section  $I(\theta)$  by

$$\sigma_1 = 2\pi \int_0^\pi I(\theta)(1 - \cos\theta) \sin\theta d\theta \quad (18)$$

and

$$\sigma_2 = 2\pi \int_0^\pi I(\theta) \sin^3\theta d\theta, \quad (19)$$

respectively. If the two atoms are different or the energy is such that symmetry effects are negligible, then these cross sections can be written in terms of the partial-wave phase shifts as follows<sup>10</sup>:

$$\sigma_1 = \frac{4\pi}{k^2} \sum_l (l+1) \sin^2(\eta_{l+1} - \eta_l) \quad (20)$$

and

$$\sigma_2 = \frac{2\pi}{k^2} \sum_l \frac{(l+1)(l+2)}{l + \frac{3}{2}} \sin^2(\eta_{l+2} - \eta_l), \quad (21)$$

where  $k^2 = 2ME$  in terms of the reduced mass  $M$  and collision energy  $E$ . Whenever a large number of partial waves contribute, which is the case in the present work,  $l$  can be treated as a continuous variable and the summations can be replaced by integrations. The integrations over  $l$  were performed by Gauss-Legendre quadrature with the interval lengths determined by the rate of variation of the phase shift (typically, 20 intervals of 10 points each were used).

The phase shifts in the semiclassical JWKB approximation with the Langer modification are given by

$$\eta_l = k \lim_{R \rightarrow \infty} \left[ \int_{R_c}^R \left( 1 - \frac{b^2}{r^2} - \frac{V(r)}{E} \right)^{1/2} dr - \int_b^R \left( 1 - \frac{b^2}{r^2} \right)^{1/2} dr \right], \quad (22)$$

where  $b = (l + \frac{1}{2})/k$  and  $R_c$  is the outermost classical turning point. For scattering not involving the very long-range shielded  $R^{-1}$  potential, the phase shift can be efficiently evaluated by converting Eq. (22) to a form suitable for Gauss-Mehler quadrature<sup>11</sup> (25 points were used). For ion-ion scattering the Debye electron shielding length is typically several orders of magnitude larger than atomic dimensions and more care, though little additional computational time, is required. The integral in the latter case was done numerically from the lower integration limit to  $R$  (a simple change of variable allows the techniques of Ref. 11 to still be used) and analytically from  $R$  to  $\infty$ , with  $R = \max(5R_c, 5b, 10)$ . At  $r > R$  the inverse  $r$  dependence in Eq. (22), with  $V(r)$  given by Eq. (1), was expanded through fifth order. We should also note that better accuracy was obtained by calculating the phase differences,  $\eta_{l'} - \eta_l$ , directly.

### B. Results for $U^+$ scattering by $U$ , $U^+$ , and $U^{2+}$

The GKR model used to obtain the potential curves works with atomic charge densities rather than wave functions, so in the case of an interaction like  $U^+ - U$ , which actually has a splitting owing to inversion symmetry, it yields an average potential. There are several gerade-ungerade pairs of potentials which arise from the  $U^+ - U$  interaction but we approximate the scattering by the average potential consistent with the charge densities described above. This potential should be a good approximation for the "hard-body" contribution to momentum transfer. The results for scattering of  $U^+$  by  $U^+$  or  $U^{2+}$ , obtained with an electron shielding length of  $10^5 a_0 (= 5.29 \times 10^{-4} \text{ cm})$ , are shown in Fig. 3. In addition to  $\sigma_1$ , the momentum-transfer (or diffusion) cross section, and  $\sigma_2$ , the viscosity cross section, we show  $\sigma_0$ , the "energy-dependent geometric" cross section. The latter cross section, defined by

$$\sigma_0 = \pi R_{c0}^2, \quad (23)$$

with  $R_{c0}$  such that

$$V(R_{c0}) = E, \quad (24)$$

is not a usual kinetic cross section but provides an interesting comparison. At low energies the behavior of the kinetic cross sections in Fig. 3

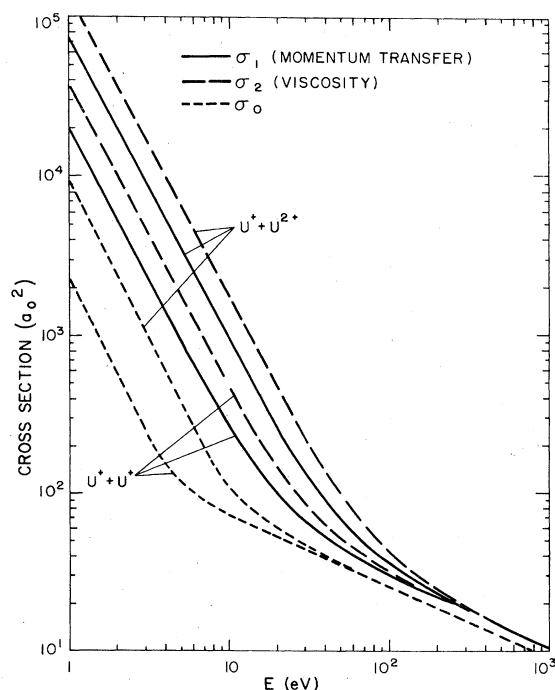


FIG. 3. Cross sections for  $U^+ + U^+$  and  $U^+ + U^{2+}$  collisions as a function of energy (center-of-mass system). See text for definition of  $\sigma_0$ . ( $1 a_0^2 \approx 0.28 \text{ \AA}^2$ ).

approaches that characteristic of Coulomb scattering; namely, the cross sections vary as  $E^{-2}$ ,  $\sigma(U^{2+} - U^+) \approx 4\sigma(U^+ - U^+)$ , and  $\sigma_2 \approx 2\sigma_1$ . As the energy increases the effect of the long-range Coulomb potential diminishes and the cross sections for  $U^+ - U^+$  and  $U^+ - U^{2+}$  collisions become similar.

The ion-ion cross sections depend, of course, on the Debye electron shielding length

$$\lambda_{De} = (k_B T_e / 4\pi e^2 n_e)^{1/2}, \quad (25)$$

where  $k_B$  is the Boltzmann constant,  $T_e$  is the electron temperature, and  $n_e$  is the electron density. Only the electrons have been assumed to be in a Boltzmann distribution. Shielding by ions is neglected in the above expression but, if important, would reduce the effective shielding length somewhat. The dependence of the momentum-transfer cross section  $\sigma_1$  on  $\lambda_{De}$  over a four-decade range is shown in Fig. 4 for  $U^+ - U^+$  scattering at four different energies. Considering that the cross sections would be infinite without shielding, the dependence is remarkably weak even at low collision energies. We may note that even though extremely large angular momenta, of the order of  $k\lambda_{De}$ , contribute weakly to the cross sections, no difficulties are encountered with the integration techniques described above.

The scattering of  $U^+$  by neutral  $U$  is qualitatively different from the ion-ion scattering.<sup>12</sup> The cross sections, assuming a polarization cutoff constant  $R_0 = 1$  [see Eq. (16)], are shown in Fig. 5. The low-energy ion-atom scattering is interpretable in terms of classical orbiting; i.e., the attractive

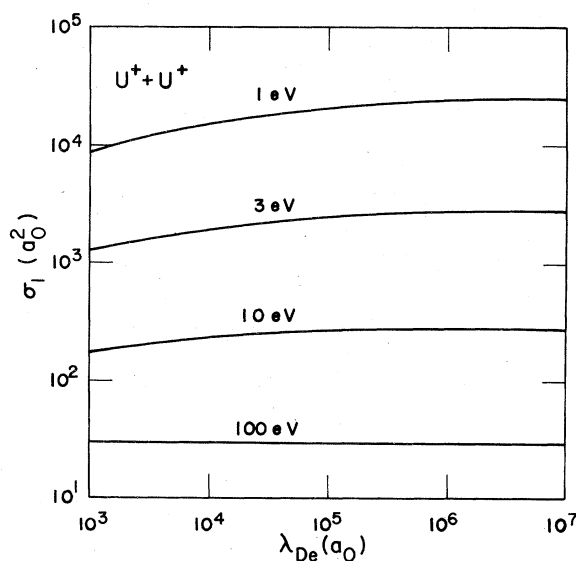


FIG. 4. Dependence of the  $U^+ + U^+$  momentum-transfer cross section on the electron shielding length at four different collision energies.

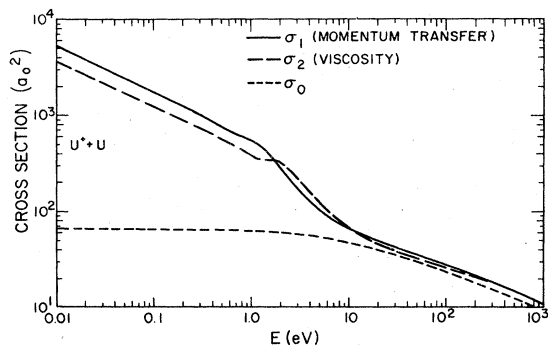


FIG. 5. Cross sections for  $U^+ + U$  collisions as a function of energy (center-of-mass system). The polarization cutoff parameter is  $R_0 = 1a_0$ . The contribution of charge transfer is not included.

potential together with the centrifugal term provide an effective potential with a barrier. Hence, at sufficiently low scattering energies there exists a critical impact parameter  $b_0$ , the "orbiting radius," at which the classical tuning point is discontinuous. For a pure polarization potential,

$$b_0 = (2\alpha/E)^{1/4} \quad (26)$$

(in a.u.) and orbiting can occur for any  $E$ . For a realistic potential,  $b_0$  depends on the short-range potential as well and orbiting is limited to collisions at energies less than about half the potential-energy well depth. This behavior can be seen in Fig. 5. At energies less than about 1 eV, the kinetic cross sections are about  $\pi b_0^2$  with the corresponding energy dependence of  $E^{-1/2}$ . This value is much larger than the energy-dependent geometric cross section which ignores the effect of centrifugal barriers. In the low-energy<sup>12</sup> limit  $\sigma_1/\sigma_2 \approx 1.43$ . Strictly speaking, the semiclassical method<sup>13</sup> is not valid for impact parameters close to  $b_0$ . Nevertheless, this treatment is expected to be accurate for the integrated cross sections.

The cross sections in the transition energy range, where the scattering switches from dominance by the polarization potential to dominance by the short-range potential, are somewhat uncertain because of the arbitrariness in the choice of the cutoff distance  $R_0$  in the polarization-potential function. The momentum-transfer cross section is shown in Fig. 6 for four choices of  $R_0$ : 0.5, 1.0, 2.0 and  $\infty$ . If polarization is neglected ( $R_0 \rightarrow \infty$ ) the cross section is much too small at low energies. On the other hand, for  $R_0 = 0.5$ , the polarization potential affects the cross section significantly even at relatively high energies ( $\approx 100$  eV), a behavior which is not physically reasonable. The choice  $R_0 = 1$  makes the cross section insensitive to small changes in  $R_0$  except in the transition region and also yields a reasonable potential-

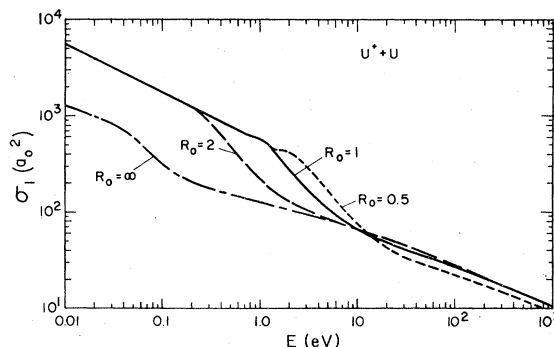


FIG. 6.  $U^+ + U$  momentum-transfer cross sections for four different polarization cutoff parameters  $R_0$ .

energy well depth (see Fig. 2).

It may be noted that in the special case of the transport cross sections,  $\sigma_1$  and  $\sigma_2$ , the semiclassical method with  $l$  treated as a continuous variable is equivalent to the classical result.<sup>12</sup> This equivalence is not general since it obviously does not hold for the non-Coulomb differential cross section  $I(\theta)$ . In any event, the method described in the present work is computationally as fast as classical calculations. Hahn *et al.*<sup>14</sup> have previously discussed quantum effects in ionized gases and calculated quantum cross sections for a shielded Coulomb potential not modified by a short-range barrier.

Molecular inversion symmetry and the associated resonant charge transfer in collisions have been neglected in the present work. At the higher energies considered resonant charge transfer will make the dominant contribution to the effective momentum-transfer cross section for collisions of  $U^+$  with  $U$  or  $U^{2+}$  (charge exchange is relatively unimportant for  $U^+ + U^+$  collisions, of course). The contribution to  $\sigma_1$  by charge transfer is given approximately by *twice* the charge-transfer cross section.<sup>15</sup> Charge transfer has little effect on the cross section  $\sigma_2$  since  $\sigma_2$  has zero weight in the backward direction. Charge transfer cross sections for  $U^+ + U$  collisions have been calculated by Sinha and Bardsley<sup>16</sup>; they obtain

$$\sigma_{tr}^{(U^+ + U)} \approx (23.8 - 2.93 \log_{10} E)^2 + 4.12 E^{-1.12},$$

where  $E$  is the center-of-mass energy in eV and  $\sigma_{tr}$  is in  $a_0^2$ . This is in fairly good agreement with the result obtained using the very simple theory of Dewangan<sup>17</sup> (fit for the energy range 1–1000 eV),

$$\sigma_{tr}^{(U^+ + U)} \approx (24.4 - 2.50 \log_{10} E)^2.$$

According to the theory of Dewangan

$$\sigma_{tr}^{(U^+ + U^{2+})} = 0.58 \sigma_{tr}^{(U^+ + U)}.$$

This result may be reasonable at energies large enough for the impact parameter method with straight-line trajectories to be valid. However, it should be viewed with caution since resonant charge transfer between  $U^+$  and  $U^{2+}$  requires a change in configuration from  $s^2$  to  $d$ , and hence the simple one-electron asymptotic theory is not really applicable.

## ACKNOWLEDGMENTS

The author is grateful to Dr. P. J. Hay for providing the relativistic Hartree-Fock charge densities, and to Dr. Hay, Dr. R. T. Pack, Dr. O. P. Judd, and Dr. C. P. Robinson for helpful discussions. This work was performed under the auspices of the U. S. Department of Energy.

\*Presently Visiting Associate Professor, Dept. of Physics, Rice Univ., Houston, Tex. 77001, on leave from Los Alamos Scientific Laboratory.

<sup>1</sup>See, e.g., D. C. Montgomery and D. A. Tidman, *Plasma Kinetic Theory* (McGraw-Hill, New York, 1964), Chap. 2.

<sup>2</sup>R. G. Gordon and Y. S. Kim, *J. Chem. Phys.* **56**, 3122 (1972).

<sup>3</sup>A. I. M. Rae, *Chem. Phys. Lett.* **18**, 574 (1973).

<sup>4</sup>For a review, see M. J. Clugston, *Adv. Phys.* **27**, 893 (1978).

<sup>5</sup>J. S. Cohen and R. T. Pack, *J. Chem. Phys.* **61**, 2372 (1974).

<sup>6</sup>V. K. Nikulin and Y. N. Tsarev, *Chem. Phys.* **10**, 433 (1975); V. K. Nikulin, *Zh. Tekh. Fiz.* **41**, 41 (1971) [*Sov. Phys.-Tech. Phys.* **16**, 28 (1971)].

<sup>7</sup>R. D. Cowan and D. C. Griffin, *J. Opt. Soc. Am.* **66**, 1010 (1976).

<sup>8</sup>A. Temkin and J. C. Lamkin, *Phys. Rev.* **121**, 788 (1961).

<sup>9</sup>K. M. S. Saxena and S. Fraga, *J. Chem. Phys.* **57**, 1800 (1972). The actual polarizability may be somewhat

larger since this calculation was done with a  $5f^4 7s^2$  rather than the actual  $5f^3 6d 7s^2$  ground-state configuration and since relativistic effects tend to reduce the binding energy of  $f$  electrons.

<sup>10</sup>N. F. Mott and H. S. W. Massey, *The Theory of Atomic Collisions*, 3rd ed. (Oxford University, London, 1965), Chap. XIX.

<sup>11</sup>J. S. Cohen, *J. Chem. Phys.* **68**, 1841 (1978).

<sup>12</sup>E. W. McDaniel and E. A. Mason, *The Mobility and Diffusion of Ions in Gases* (Wiley, New York, 1973), Chap. 5 and Appendix I.

<sup>13</sup>K. W. Ford, D. L. Hill, M. Wakano, and J. A. Wheeler, *Ann. Phys. (N.Y.)* **7**, 239 (1959); K. W. Ford and J. A. Wheeler, *ibid.* **7**, 259 (1959).

<sup>14</sup>H. Hahn, E. A. Mason, and F. J. Smith, *Phys. Fluids* **14**, 278 (1971).

<sup>15</sup>A. Dalgarno, *Philos. Trans. R. Soc. London A* **250**, 426 (1958).

<sup>16</sup>S. Sinha and J. N. Bardsley, *Phys. Rev. A* **14**, 104 (1976).

<sup>17</sup>D. P. Dewangan, *J. Phys. B* **6**, L20 (1973).